

1 **Amplified North Atlantic warming in the late Pliocene by changes in**
2 **Arctic gateways**

3

4 **Bette L. Otto-Bliesner¹, Alexandra Jahn², Ran Feng¹, Esther C. Brady¹, Aixue Hu¹,**

5 and Marcus Löfverström¹

6 ¹Climate and Global Dynamics Laboratory, National Center for Atmospheric Research,
7 Boulder, CO 80305, USA.

8 ²Dept. of Atmospheric and Oceanic Sciences and Institute of Arctic and Alpine Research,
9 Univ. of Colorado Boulder, Boulder, CO 80309, USA.

10 Corresponding Author: Bette L. Otto-Bliesner (ottobli@ucar.edu)

11

12

13 **Key Points:**

14 • Closure of Arctic gateways in a new reconstruction of mid-Piacenzian
15 paleogeography reduces simulated Arctic freshwater exports to the North Atlantic
16 and enhances the AMOC

17 • Simulated regional patterns of temperature show better correspondence with
18 proxy-indicated warm sea surface temperatures in the North Atlantic

19 • The climatic response to the closure of Arctic gateways is not a linear
20 combination to the closure of the individual straits.

21

22 **An edited version of this paper was published by AGU. Copyright (2016) American**
23 **Geophysical Union**

24 Published as: Otto-Bliesner, B. L., A. Jahn, R. Feng, E. C. Brady, A. Hu, and M.
25 Löfverström (2016), Amplified North Atlantic warming in the late Pliocene by changes
26 in Arctic gateways, *Geophys. Res. Lett.*, 44, doi:10.1002/2016GL071805.

27

28

29 **Abstract**

30 Under previous reconstructions of late Pliocene boundary conditions, climate models
31 have failed to reproduce the warm sea surface temperatures reconstructed in the North
32 Atlantic. Using a reconstruction of mid-Piacenzian paleogeography that has the Bering
33 Strait and Canadian Arctic Archipelago Straits closed, however, improves the simulation
34 of the proxy-indicated warm sea surface temperatures in the North Atlantic in the
35 Community Climate System Model. We find that the closure of these small Arctic
36 gateways strengthens the Atlantic Meridional Overturning Circulation, by inhibiting
37 freshwater transport from the Pacific to the Arctic Ocean and from the Arctic Ocean to
38 the Labrador Sea, leading to warmer sea surface temperatures in the North Atlantic. This
39 indicates that the state of the Arctic gateways may influence the sensitivity of the North
40 Atlantic climate in complex ways, and better understanding of the state of these Arctic
41 gateways for past time periods are needed.

42 **1 Introduction**

43 Data reconstructions and Pliocene Model Intercomparison Project Phase 1
44 [PlioMIP1] climate model simulations of the Pliocene sea surface temperatures (SSTs),
45 specifically during the mid-Piacenzian [mP, 3.264 – 3.025 Ma], are in good agreement in
46 most regions except at sites in the North Atlantic [Dowsett *et al.*, 2013]. Higher levels of
47 ocean heat transport, based on micropaleontological evidence [Dowsett *et al.*, 1992] and
48 carbon isotopic composition of marine organic matter [Raymo *et al.*, 1996], have been
49 invoked to explain the origin of this Pliocene warmth, but coupled climate models have
50 failed to consistently reproduce the magnitude or agree even on the sign of the change in
51 the Atlantic Meridional Overturning Circulation (AMOC) [Haywood and Valdes, 2004;
52 Zhang *et al.*, 2013]. Furthermore, an alternate explanation, which invokes the higher
53 reconstructed concentrations of atmospheric carbon dioxide (CO₂) during the Pliocene
54 [Budyko *et al.*, 1985; Crowley, 1991], is also not sufficient and calls into question
55 whether coupled climate models adequately simulate polar amplification.

56 Experiments have also explored the AMOC responses to replacing the Barents
57 Sea with land [Hill, 2015], a deepening of the sills along the eastern and western limbs of
58 the Greenland-Scotland-Iceland ridge [Robinson *et al.*, 2011], and an extended drainage
59 basin of the Hudson Bay and Baltic rivers [Hill, 2015]. Among these changes, only
60 changes to the Greenland-Scotland-Iceland ridge have led to a significant strengthening
61 of the AMOC. A new reconstruction of mP paleogeography [Dowsett *et al.*, 2016]
62 includes closure of the Bering and Canadian Arctic Archipelago Straits. The impacts of
63 the representation of these gateways and influences on pathways of present-day ocean
64 currents have been investigated with ocean-only [e.g. Wadley and Bigg, 2002] and
65 coupled ocean-sea ice models [e.g. Komuro and Hasumi, 2005]. Recent studies have also
66 investigated the climate-system response to the closure of Bering Strait [e.g. Hu *et al.*,
67 2015]. However, the climate response to both ocean gateways closed during the Pliocene
68 has yet to be explored.

69 Here we conduct a series of medium-resolution, coupled atmosphere-ocean-sea
70 ice-land simulations to better understand the North Atlantic climate response (particularly
71 the AMOC and sea-surface temperature field) to the configuration of open and closed

72 ocean gateways in the Bering Strait and the Canadian Arctic Archipelago. We quantify
73 the changes to freshwater transport to the North Atlantic with closure of these gateways
74 and subsequent impacts on the AMOC. The new simulation compares favorably to proxy
75 reconstructions of North Atlantic temperatures. This is important, as the mP warm period
76 has been suggested as a geologic example for the long-term response of the future Earth
77 to present levels of global atmospheric CO₂.

78 **2 Model and Experimental Design**

79 To identify the sensitivity of the late Pliocene climate to uncertainties in
80 reconstructions of the Arctic Ocean gateways, we conducted five coupled climate
81 simulations with the Community Climate System Model version 4 (CCSM4) [Methods,
82 Text S1] [Gent *et al.*, 2011]. The baseline Pliocene simulation uses the standard
83 PlioMIP1 forcing protocol: atmospheric CO₂ set to 405 ppmv (parts per million by
84 volume) and the Pliocene Research, Interpretation, and Synoptic Mapping, Version 3
85 (PRISM3) vegetation, ice sheets, and topography [Haywood *et al.*, 2011; Rosenbloom *et*
86 *al.*, 2013]. The land-sea geography is kept at its modern configuration except for the
87 filling of Hudson Bay. The updated PRISM4 mP paleo-environmental reconstruction,
88 which considers change in dynamic topography associated with mantle flow and glacial
89 isostatic adjustment due to Piacenzian ice loading and will be used in PlioMIP2 (centered
90 on an interglacial peak MIS KM5c: 3.205 Ma), closes the Bering Strait (BS) and the
91 straits through the Canadian Arctic Archipelago (CAA: Northwest Passage and Nares
92 Strait) [Haywood *et al.*, 2016b]. We conduct three sensitivity simulations, for comparison
93 to our baseline PlioMIP1 simulation and a preindustrial simulation [PI with 1850
94 conditions]: (1) only the BS closed, (2) only the CAA closed, and (3) both the BS and
95 CAA closed. The first two sensitivity simulations allow us to assess the linearity of the
96 effects of the individual straits on the Arctic and North Atlantic.

97 **3 Proxy Reconstructions**

98 The model simulations are compared to the reconstructions of North Atlantic SSTs
99 compiled by Dowsett *et al.*, 2012, 2013 (Table S1). The confidence level of the proxy-
100 data records were evaluated by these authors based on semi-quantitative measure of
101 confidence accounting for quality of the age control of the samples at each site, number
102 of samples at each site, fossil preservation and abundance, reliability of proxy method or
103 technique used; we retain only records with high to very high confidence level in this
104 study. The model-proxy comparison is conducted on the anomalies of the simulated
105 Pliocene and preindustrial temperatures. In order to ensure the consistency of model-
106 proxy data comparison, published proxy anomalies (reference to modern) are corrected
107 with preindustrial minus present-day anomalies (Rayner *et al.*, 2003; Reynolds *et al.*,
108 2002).

109 **4 Results**

110 **4.1 Impacts of closing Arctic gateways on North Atlantic Ocean**

111 CCSM4 reasonably reproduces observed SST and sea surface salinity (SSS) in the
112 North Atlantic with warm and saline conditions extending across the basin south of

113 ~45°N and northward into the eastern Greenland-Iceland-Norwegian (GIN) Sea (Fig. S1).
114 Cold and fresher conditions extend from the Fram Strait southward along the eastern
115 Greenland coast to the Labrador Sea. The baseline PlioMIP1 simulation is warmer and
116 saltier in the North Atlantic than the PI simulation (Fig. 1). In the PI and PlioMIP1
117 simulations, deep-water formation extends from the Labrador Sea to Irminger Sea, and
118 the Greenland-Iceland-Norwegian Seas, similar as in observations (Figs. 1 and S1, e.g.,
119 Smethie et al., 2000; Danabasoglu et al., 2012). The maximum AMOC in the PlioMIP1
120 simulation is indistinguishable from the PI control (Fig. 2), also the case in PlioMIP1
121 simulations by several other models [Zhang et al., 2013]. Areal sea ice extent in the
122 CCSM4 PlioMIP1 simulation decreases in the Arctic as compared to PI (Fig. S2) but
123 persists through the summer [Rosenbloom et al., 2013].

124 With a closed Bering Strait at the Pliocene, saltier water in the Labrador and GIN
125 Seas favors increased deep-water formation in both regions (Fig. 1). The AMOC
126 strengthens by about 2.5 Sv and meridional heat transport (MHT) convergence in the
127 Atlantic between 40 – 60°N increases by 0.036 PW, or 10% as compared to the PlioMIP1
128 simulation with the BS open (Fig. 2). The strengthened AMOC is consistent with
129 modeling results for modern [Goosse et al., 1997; Wadley and Bigg, 2002] and
130 Quaternary [Hu et al., 2015] ocean circulations for a closed BS. Annual sea ice
131 concentrations are reduced by up to 15% in the waters west of Greenland (including
132 Baffin Bay, the Davis Strait, and Labrador Sea) and east of Greenland (including the East
133 Greenland Current region and in the Barents Sea) as compared to the PlioMIP1
134 simulation (Fig. S2).

135 Closure of only the CAA straits, on the other hand, results in a significant
136 freshening and cooling of the Labrador and GIN seas (Fig. 1) and thus a large expansion
137 of sea ice in these basins (Fig. S2), as compared to the PlioMIP1 simulation. Deep-water
138 formation is shutdown except in the eastern North Atlantic (Fig. 1), resulting in a
139 reduction of the AMOC by about 5 Sv or 20% (Fig. 2) and a decrease of MHT
140 convergence in the Atlantic between 40 – 60°N of -0.017 PW or -5% as compared to the
141 PlioMIP1 simulation with the CAA straits open. This contrasts with results from previous
142 studies using a low-resolution ocean model [Wadley and Bigg, 2002] and an ocean model
143 with flux corrections [Goosse et al., 1997], but it is consistent with results from an ocean-
144 sea ice model [Komuro and Hasumi, 2005].

145 With the closure of both the Bering and Canadian Arctic Archipelago straits, there
146 is a freshening of and decreased deep-water formation in the Norwegian Sea (Fig. 1), and
147 a displacement of the region of deepwater formation southeastward into the Irminger Sea
148 and the subpolar North Atlantic, resulting in more saline water emanating from the
149 Labrador Sea even compared to the closed BS case. The model responds with an even
150 greater strengthening of the AMOC (~4.5 Sv or 18%), approximately doubling the
151 response with only the Bering Strait closed. As compared to the closed BS case, the
152 strengthening of the AMOC is primarily confined to between 40 and 60°N (Fig. 2). MHT
153 convergence in this latitudinal band increases by 0.098 PW or 30% as compared to the
154 PlioMIP1 simulation. Sea ice has a dipole response, with large decreases west of
155 Greenland and increase from the tip of Greenland to the northern North Atlantic (Fig.
156 S2).

157 4.2 A mechanism for responses

158 The simulated responses can be understood by changes in the Arctic freshwater
159 (liquid and sea ice) transports and subsequent effects on the SST, SSS, and deep-water
160 formation in the North Atlantic. At present [Aagaard and Carmack, 1989] and in the
161 PlioMIP1 simulation, relatively fresh seawater is transported through the Bering Strait
162 into the Arctic, with additional freshwater being added to the Arctic Ocean through river
163 runoff and net precipitation (Fig. 3, Table S2). This freshwater is then exported from the
164 Arctic to the North Atlantic via two routes. The short route is through the Canadian
165 Arctic Archipelago straits (Northwest Passage and Nares Strait) into Baffin Bay and out
166 along the northeast coast of the Canadian Arctic. A major portion of the Pacific water
167 transported through the Bering Strait leaves the Arctic through the straits of the Canadian
168 Arctic Archipelago [Jahn *et al.*, 2010]. The long route is through the Fram Strait, with a
169 large contribution from sea ice export. Previous work has shown that the CCSM4
170 represents the Arctic freshwater fluxes reasonably well in present-day simulations [Jahn
171 *et al.*, 2012], and that changes in the Arctic freshwater export affect the simulated deep
172 convection in the North Atlantic in the CCSM4 more strongly than SST changes [Jahn
173 and Holland, 2013].

174 With a closed Bering Strait in the Pliocene, the total freshwater (liquid and solid,
175 FW) transported to the North Atlantic through the Fram Strait decreases by about 39%
176 and through the CAA Straits by 36%, with a total reduction of the Arctic FW export of
177 about 30% (Fig. 3, Table S2), resulting in a saltier Labrador and GIN Seas (Fig. 1). With
178 an open BS but closed CAA, the total FW export stays about the same as in the baseline
179 Pliocene experiment, but all freshwater must be exported through the Fram Strait (Fig. 3,
180 Table S2). This more-than-doubled FW export by the long route explains the significant
181 freshening and cooling of the Labrador and GIN seas (Fig. 1), increased sea ice cover
182 (Fig. S2) and sea ice melt, and a shutdown of deep-water formation except in the eastern
183 North Atlantic (Fig. 1).

184 For the mP simulation with closed BS and closed CAA straits, Arctic FW is
185 transported entirely through the Fram Strait and is sourced only from the local Arctic FW
186 budget (P-E+R), as no Pacific FW is entering the Arctic. Compared to the baseline
187 PlioMIP1 experiment, this leads to a 30% reduction of the total FW export from the
188 Arctic, similar to the closed BS case. In contrast to the closed BS case, however, this
189 reduction is entirely due to a 36% decrease in the total liquid FW export from the Arctic
190 (Table S2). The total sea ice export stays at the same level as in the PlioMIP1 simulation.
191 As all FW now leaves the Arctic east of Greenland, it leads to a freshening of and
192 decreased deep-water formation in the Norwegian Sea (Fig. 1). At the same time, the
193 strongly reduced total liquid FW export together with the cutoff of the short export route
194 through the CAA results in a more saline Labrador and south Greenland Sea with
195 increased deep convection, even compared to the closed BS case (Fig. 1). The stronger
196 AMOC in the mP simulation with closed BS and closed CAA straits is therefore due to
197 the phase and pathway of the Arctic FW export, rather than being a linear combination of
198 the AMOC response in the individual closure cases of the Bering and CAA straits (Fig.
199 2).

200 4.3 Impact on North Atlantic and Arctic temperatures

201 Our PlioMIP1 simulation, with open BS and CAA straits, has a 1.9°C increase in
202 global mean annual temperature compared to the PI control, with a polar amplification of
203 ~3 times the global warming [Rosenbloom *et al.*, 2013]. Compared to proxy data, the
204 PlioMIP1 simulation underestimates the reconstructed warm mid-latitudes (40 – 60°N) of
205 the North Atlantic (Fig. 4). The model simulates on average 1.4°C warming (range 0.7 to
206 1.8°C) at mid-latitude proxy sites characterized as high and very high confidence
207 [Dowsett *et al.*, 2012] relative to the PI simulation (Fig. 4, Table S1), while the warming
208 is 5.1°C (range -0.2 to 8.8°C) derived from proxy reconstructions. This data model
209 mismatch is worsened in the closed CAA experiment with an average cooling of 0.8°C
210 (range -3.0 to 0.8°C), but is improved by closing the BS and further by closing both the
211 BS and the CAA straits, featuring a 2.4°C (range 1.8 to 4.0°C) and 3.2°C (range 1.9 to
212 5.5°C) warming, respectively (Table S1).

213 With the new mP PRISM4 reconstruction of Arctic gateways, the model still
214 underestimates pan-Arctic (greater than 60°N) warming. None of the simulations capture
215 the strong warming reconstructed for ODP 907 near Iceland, a site assessed to be high
216 confidence (Table S1). Other pan-Arctic sites provide less confident temperature
217 estimates due to dating and calibration uncertainties. In particular, the large age range of
218 many terrestrial records mean that the proxy mean annual temperatures may represent
219 periods in the Pliocene with higher CO₂ than prescribed in the CCSM4 Pliocene
220 simulations and/or could represent periods within the Pliocene with high summer
221 insolation anomalies in the Arctic [Haywood *et al.*, 2016a; Prescott *et al.*, 2014; R. Feng,
222 pers. comm.]. Similarly, other differences in the paleogeography [Hill, 2015] or
223 bathymetry in the North Atlantic [Robinson *et al.*, 2011] from modern could be
224 important. Previous modeling has shown that an ice-free Arctic in the summer provides a
225 better match to the proxy temperature data [Ballantyne *et al.*, 2013; Howell *et al.*, 2016].
226 Whether this speaks to models such as CCSM4 underestimating the sensitivity of Arctic
227 sea ice to warming, or the need to include the chemistry-climate feedbacks [Unger and
228 Yue, 2014] associated with the changed vegetation not commonly included in
229 paleoclimate simulations, remains an open question.
230

231 4.4 Implications for Pliocene Greenland Ice Sheet

232 Ice-rafted detritus records suggest a significant expansion of the Greenland ice
233 sheet (GrIS) during the M2 glacial event (~3.3 Ma) [Flesche Kleiven *et al.*, 2002;
234 Bierman *et al.*, 2016] that temporarily punctuated the relatively stable warm climate of
235 the late Pliocene. The driver of this glaciation is not well understood, though insolation
236 and CO₂ variations are thought to have played important roles for the ice sheet formation
237 [Contoux *et al.*, 2015; Dolan *et al.*, 2015; Koenig *et al.*, 2015]. The results presented here
238 suggest that the cold SST feedback (when only closing the CAA straits but leaving BS
239 open) may have been important for this transition as well, and possibly also for
240 subsequent glaciations in the Pleistocene. These results highlight the importance of
241 further studies with coupled climate-ice-sheet models for understanding GrIS responses
242 to the Arctic gateway configurations.

243

244 **5 Conclusions**

245 Our simulations show that closure of the relatively small Arctic gateways
246 critically influences the AMOC, by inhibiting freshwater transport from the Pacific to the
247 Arctic Ocean and from the Arctic Ocean to the Labrador and Greenland-Iceland-
248 Norwegian (GIN) Seas. The net result is a stronger AMOC and an improved simulation
249 of the proxy-indicated warm SSTs across the North Atlantic from south of Greenland to
250 the British Isles with closure of both the Bering Strait and straits in the Canadian Arctic
251 Archipelago. These results indicate the need to have better assess the climate impact of
252 these Arctic gateways when using models in comparison to data for past time periods.

253 The Pliocene has been used as a geologic analogue to assess the long-term climate
254 response to modern CO₂ levels. Pliocene proxy reconstructions consistently show greater
255 high latitude warmth, and possibly more sensitive climate [Pagani *et al.*, 2010] than
256 simulated by state-of-the-art Earth system models [Haywood *et al.*, 2013]. Our results
257 indicate that the state of the Arctic gateways may influence the sensitivity of the North
258 Atlantic climate in complex ways, making the Pliocene a better process than geologic
259 analogue to study the ability of models to realize the full sensitivity to processes and
260 feedbacks that may affect the Earth system sensitivity in the future.

261 **Acknowledgments and Data**

262 We thank the CESM scientists and software engineers for the development of the
263 Community Earth System Model, Nan Rosenbloom for setting up and running
264 simulations, and the PRISM group for the development of the Pliocene boundary
265 conditions. The National Center for Atmospheric Research (NCAR) is sponsored by the
266 U.S. National Science Foundation (NSF). B.L.O.-B. and E.C.B. also acknowledge the
267 support of NSF-EAR award 1237211. A.J.'s contribution is supported by NSF-OPP
268 award 1504348. R.F. is supported by NSF-PLR award 1418411. A.H. is supported by the
269 U.S. Department of Energy (DOE), Office of Science (BER) cooperative agreement DE-
270 FC02-97ER62402 and M.L. by DOE-BER award DE-SC0012606. Computing resources
271 (ark:/85065/d7wd3xhc) were provided by the Climate Simulation Laboratory at NCAR's
272 Computational and Information Systems Laboratory, sponsored by the National Science
273 Foundation and other agencies. The model data are archived on the High-Performance
274 Storage System at the NCAR-Wyoming Supercomputing Center and are available from
275 the authors on request (ottobli@ucar.edu).

276

277

278

279

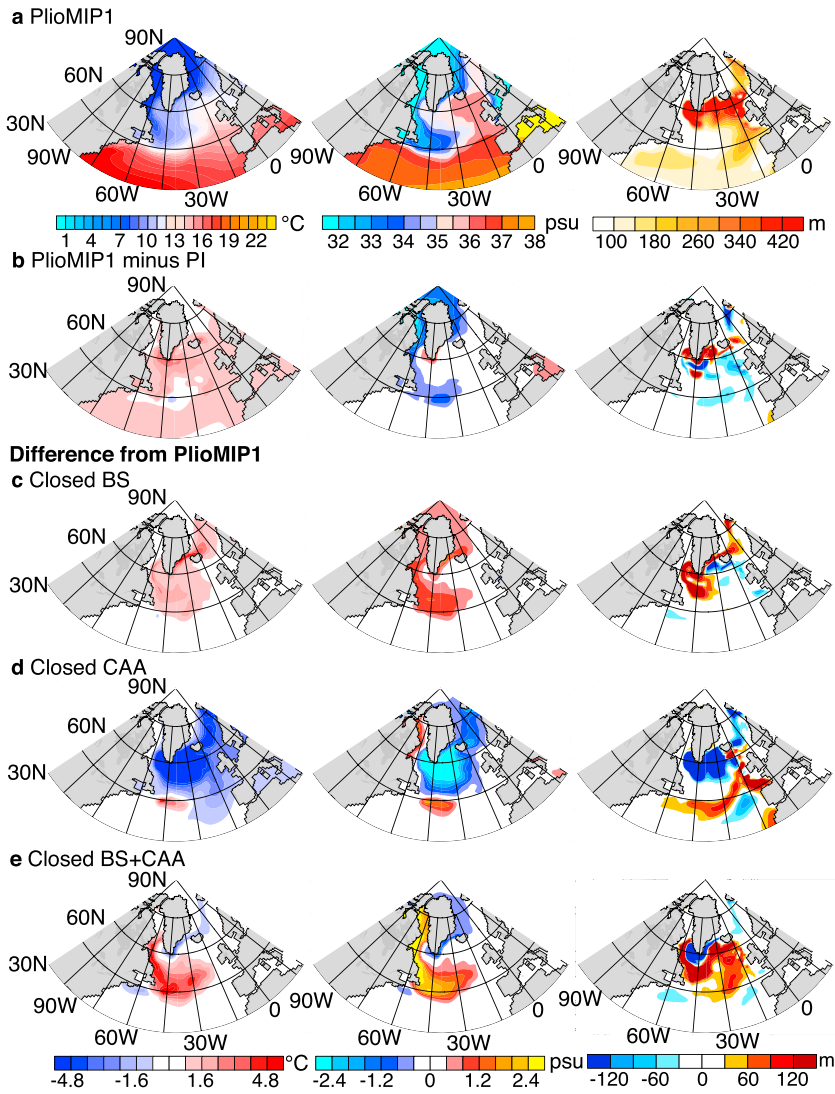
280

281

282

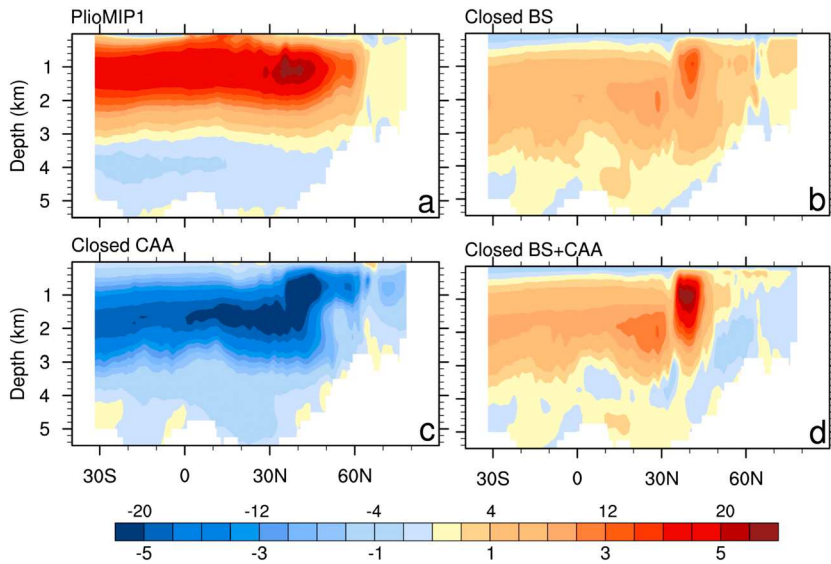
283

284 **Figures**



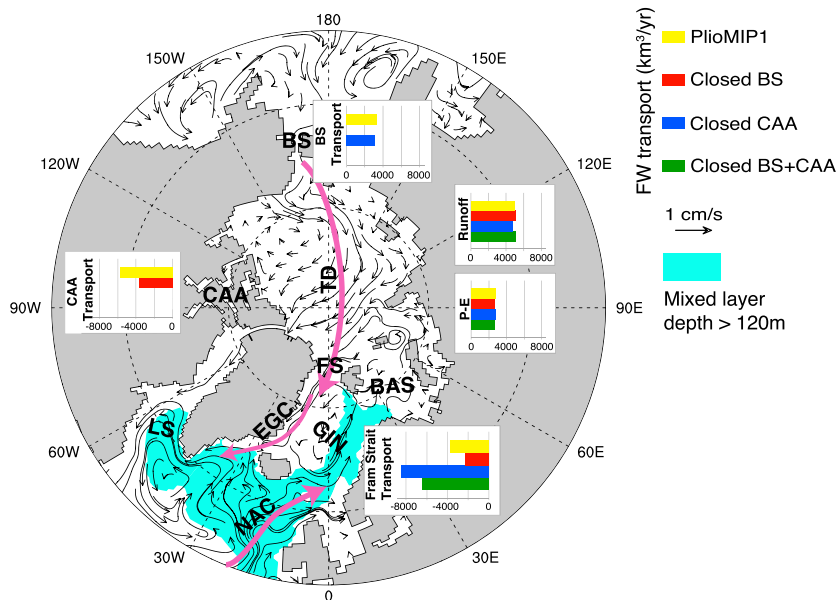
285

286 **Figure 1. Comparison of SST (left), SSS (middle) and mixed layer depth (MLD,**
287 **right). Panel a, annual-mean SST (°C), annual-mean SSS (psu), winter (December to**
288 **February) MLD in the PlioMIP1 simulation. Panel b, PlioMIP1 minus PI changes in SST,**
289 **SSS, and MLD. Panels c, d, e, changes in SST, SSS and MLD with respect to the**
290 **PlioMIP1 simulation for the Closed BS, Closed CAA, and Closed BS+CAA experiments,**
291 **respectively.**



292

293 **Figure 2. Comparison of AMOC in Pliocene simulations.** a, Annual-mean AMOC
 294 (Sv) from PlioMIP1 simulation. Positive and negative contours indicate clockwise and
 295 counterclockwise circulation, respectively. b, c, d, Change in the AMOC as compared to
 296 the PlioMIP1 simulation for the Closed BS, Closed CAA, and Closed BS+CAA
 297 experiments, respectively. Top numbers in colorbar are used by panel a, and bottom
 298 numbers are used by panels b,c,d.



299

300 **Figure 3. Arctic Ocean freshwater fluxes into and out of Arctic Ocean.** Streamlines
 301 represent ocean surface circulation in the PlioMIP1 simulation. Net freshwater (solid plus
 302 liquid, in km^3/yr) input (positive values) and export (negative values) are shown for the

303 Pliocene simulations. Shaded blue area shows the region where winter ocean mixed layer
 304 depths are greater than 120m in the PlioMIP1 simulation. Other regions are labeled as
 305 BAS, Barents Sea; BS, Bering Strait; CAA, Canadian Arctic Archipelago; EGC, East
 306 Greenland Current; FS, Fram Strait; GIN, Greenland-Iceland-Norwegian Sea; LS,
 307 Labrador Sea; NAC, North Atlantic Current; TD, Transport Drift. 1 Sv equals $10^6 \text{ m}^3/\text{s}$
 308 and $3.1536 \times 10^4 \text{ km}^3/\text{yr}$.

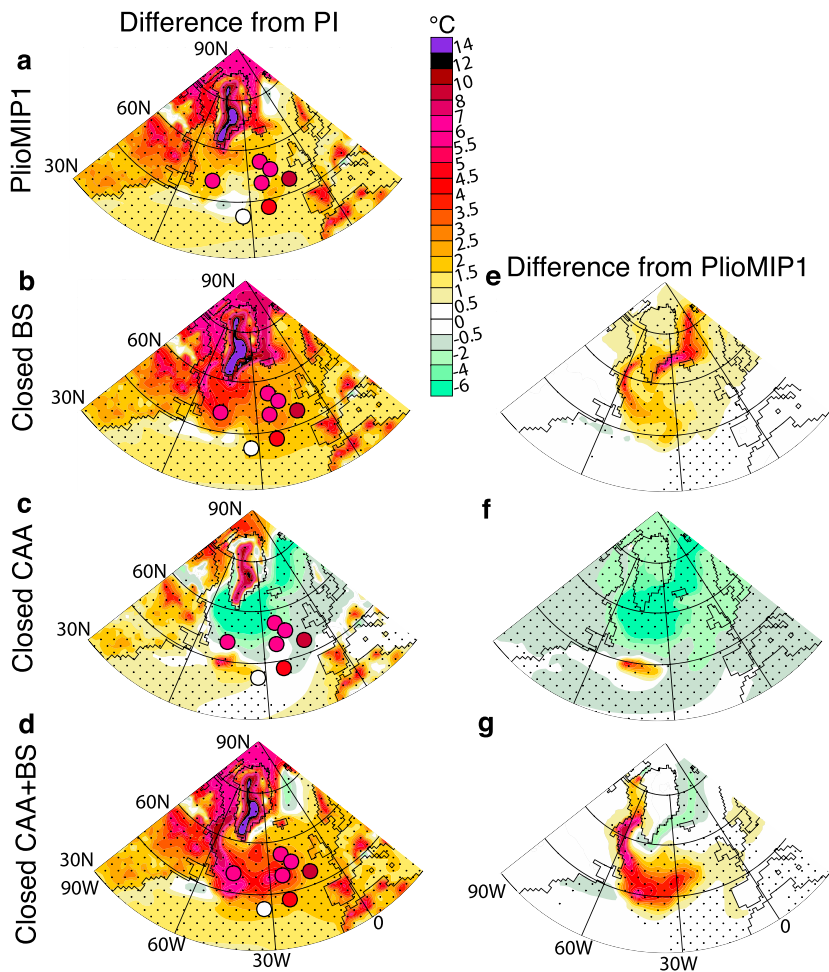


Figure 4. Annual surface temperature change (°C) in Pliocene simulations (contours) and proxy-data reconstructions (filled circles). Panels a-d, Change as compared to CCSM4 preindustrial simulation. Information about data points is presented in Table S1. Panels e-g, changes with respect to the PlioMIP1 simulation. Areas with differences significant above 99% (from Student's t-test) are dotted.

316 **References**

317 Aagaard, K., and E. C. Carmack (1989), The role of sea ice and other fresh-water in the
318 arctic circulation, *J. Geophys. Res. Oceans*, 94(C10), 14485-14498,
319 doi:10.1029/JC094iC10p14485.

320 Antonov, J. I., D. Seidov, T. P. Boyer, R. A. Locarnini, A. V. Mishonov, H. E. Garcia, O.
321 K. Baranova, M. M. Zweng, and D. R. Johnson (2010), World Ocean Atlas 2009,
322 Volume 2: Salinity. S. Levitus, Ed. NOAA Atlas NESDIS 69, U.S. Government
323 Printing Office, Washington, D.C.

324 Ballantyne, A. P., Y. Axford, G. H. Miller, B. L. Otto-Bliesner, N. Rosenbloom, and J. W.
325 C. White (2013), The amplification of Arctic terrestrial surface temperatures by
326 reduced sea-ice extent during the Pliocene, *Paleogeogr. Paleoceanogr. Paleoclimatol.*,
327 386, 59-67, doi:10.1016/j.palaeo.2013.05.002.

328 Ballantyne, A. P., D. R. Greenwood, J. S. S. Damste, A. Z. Csank, J. J. Eberle, and N.
329 Rybczynski (2010), Significantly warmer Arctic surface temperatures during the
330 Pliocene indicated by multiple independent proxies, *Geology*, 38(7), 603-606,
331 doi:10.1130/g30815.1.

332 Bierman, P. R., J. D. Shakun, L. B. Corbett, S. R. Zimmerman, and D. H. Rood (2016), A
333 persistent and dynamic East Greenland Ice Sheet over the past 7.5 million years,
334 *Nature*, 540, 256-260, doi:10.1038/nature20147.

335 Budyko, M. I., A. B. Ronov, and A. L. Yanshin (1985), *The History of the Earth's
336 Atmosphere*, 139 pp pp., English translation: Springer, Berlin, 1987, Leningrad,
337 Gidrometeoizdat.

338 Contoux, C., C. Dumas, G. Ramstein, A. Jost, and A. M. Dolan (2015), Modelling
339 Greenland ice sheet inception and sustainability during the Late Pliocene, *Earth
340 Planet. Sci. Lett.*, 424, 295-305, doi:10.1016/j.epsl.2015.05.018.

341 Crowley, T. J. (1991), Modeling Pliocene warmth, *Quat. Sci. Rev.*, 10(2-3), 275-282,
342 doi:10.1016/0277-3791(91)90025-p.

343 Danabasoglu, G., S. C. Bates, B. P. Briegleb, S. R. Jayne, M. Jochum, W. G. Large, S.
344 Peacock, and S. G. Yeager, 2012: The CCSM4 ocean component. *J. Climate*, 25,
345 1361–1389

346 Dolan, A. M., A. M. Haywood, S. J. Hunter, J. C. Tindall, H. J. Dowsett, D. J. Hill, and S.
347 J. Pickering (2015), Modelling the enigmatic Late Pliocene Glacial Event -
348 Marine Isotope Stage M2, *Global Planet. Change*, 128, 47-60,
349 doi:10.1016/j.gloplacha.2015.02.001.

350 Dowsett, H., et al. (2016), The PRISM4 (mid-Piacenzian) palaeoenvironmental
351 reconstruction, *Clim. Past*, 12, 1519-1538, doi:10.5194/cp-12-1519-2016.

352 Dowsett, H. J., T. M. Cronin, R. Z. Poore, R. S. Thompson, R. C. Whatley, and A. M.
353 Wood (1992), Micropaleontological evidence for increased meridional heat-
354 transport in the north-Atlantic ocean during the Pliocene, *Science*, 258(5085),
355 1133-1135, doi:10.1126/science.258.5085.1133.

356 Dowsett, H. J., et al. (2013), Sea Surface Temperature of the mid-Piacenzian Ocean: A
357 Data-Model Comparison, *Sci. Rep.* 3(8), doi:10.1038/srep02013.

358 Dowsett, H. J., et al. (2012), Assessing confidence in Pliocene sea surface temperatures
359 to evaluate predictive models, *Nat. Clim. Change*, 2(5), 365-371,
360 doi:10.1038/nclimate1455.

361 Flesche Kleiven, H., E. Jansen, T. Fronval, and T. M. Smith (2002), Intensification of
362 Northern Hemisphere glaciations in the circum Atlantic region (3.5-2.4 Ma) - ice-
363 rafted detritus evidence, *Paleogeogr. Paleoclimatol. Paleoecol.*, 184, 213-223.

364 Gent, P. R., et al. (2011), The Community Climate System Model Version 4, *J. Clim.*,
365 24(19), 4973-4991, doi:10.1175/2011jcli4083.1.

366 Goosse, H., T. Fichefet, and J. M. Campin (1997), The effects of the water flow through
367 the Canadian Archipelago in a global ice-ocean model, *Geophys. Res. Lett.*,
368 24(12), 1507-1510, doi:10.1029/97gl01352.

369 Haywood, A. M., H. J. Dowsett, and A. M. Dolan (2016a), Integrating geological
370 archives and climate models for the mid-Pliocene warm period, *Nat. Commun.*, 7,
371 doi:10.1038/ncomms10646.

372 Haywood, A. M., et al. (2016b), The Pliocene Model Intercomparison Project (PlioMIP)
373 Phase 2: scientific objectives and experimental design, *Clim. Past*, 12(3), 663-675,
374 doi:10.5194/cp-12-663-2016.

375 Haywood, A. M., H. J. Dowsett, M. M. Robinson, D. K. Stoll, A. M. Dolan, D. J. Lunt, B.
376 Otto-Bliesner, and M. A. Chandler (2011), Pliocene Model Intercomparison
377 Project (PlioMIP): experimental design and boundary conditions (Experiment 2),
378 *Geosci. Model Dev.*, 4(3), 571-577, doi:10.5194/gmd-4-571-2011.

379 Haywood, A. M., et al. (2013), Large-scale features of Pliocene climate: results from the
380 Pliocene Model Intercomparison Project, *Clim. Past*, 9(1), 191-209,
381 doi:10.5194/cp-9-191-2013.

382 Haywood, A. M., and P. J. Valdes (2004), Modelling Pliocene warmth: contribution of
383 atmosphere, oceans and cryosphere, *Earth Planet. Sci. Lett.*, 218(3-4), 363-377,
384 doi:10.1016/s0012-821x(03)00685-x.

385 Hill, D. J. (2015), The non-analogue nature of Pliocene temperature gradients, *Earth
386 Planet. Sci. Lett.*, 425, 232-241, doi:10.1016/j.epsl.2015.05.044.

387 Howell, F. W., et al. (2016), Arctic sea ice simulation in the PlioMIP ensemble, *Clim.
388 Past*, 12(3), 749-767, doi:10.5194/cp-12-749-2016.

389 Hu, A. X., G. A. Meehl, W. Q. Han, B. Otto-Bliesner, A. Abe-Ouchi, and N. Rosenbloom
390 (2015), Effects of the Bering Strait closure on AMOC and global climate under
391 different background climates, *Prog. Oceanogr.*, 132, 174-196,
392 doi:10.1016/j.pocean.2014.02.004.

393 Jahn, A., and M. M. Holland (2013), Implications of Arctic sea ice changes for North
394 Atlantic deep convection and the meridional overturning circulation in CCSM4-
395 CMIP5 simulations, *Geophys. Res. Lett.*, 40(6), 1206-1211, doi:10.1002/grl.50183.

396 Jahn, A., et al. (2012), Late-twentieth-century simulation of Arctic sea ice and ocean
397 properties in the CCSM4, *J. Clim.*, 25(5), 1431-1452, doi:10.1175/jcli-d-11-
398 00201.1.

399 Jahn, A., B. Tremblay, L. A. Mysak, and R. Newton (2010), Effect of the large-scale
400 atmospheric circulation on the variability of the Arctic Ocean freshwater export,
401 *Clim. Dyn.*, 34(2-3), 201-222, doi:10.1007/s00382-009-0558-z.

402 Koenig, S. J., et al. (2015), Ice sheet model dependency of the simulated Greenland Ice
403 Sheet in the mid-Pliocene, *Clim. Past*, 11(3), 369-381, doi:10.5194/cp-11-369-
404 2015.

405 Komuro, Y., and H. Hasumi (2005), Intensification of the Atlantic deep circulation by the
406 Canadian Archipelago throughflow, *J. Phys. Oceanogr.*, 35(5), 775-789,
407 doi:10.1175/jpo2709.1.

408 Locarnini, R. A., A. V. Mishonov, J. I. Antonov, T. P. Boyer, H. E. Garcia, O. K.
409 Baranova, M. M. Zweng, and D. R. Johnson (2010), World Ocean Atlas 2009,
410 Volume 1: Temperature. S. Levitus, Ed. NOAA Atlas NESDIS 68, U.S.
411 Government Printing Office, Washington, D.C.

412 Monterey G. and S. Levitus (1997), Seasonal Variability of Mixed Layer Depth for the
413 World Ocean, NOAA Atlas NESDIS 14, U.S. Government Printing Office,
414 Washington, D.C.

415 Pagani, M., Z. H. Liu, J. LaRiviere, and A. C. Ravelo (2010), High Earth-system climate
416 sensitivity determined from Pliocene carbon dioxide concentrations, *Nat. Geosci.*,
417 3(1), 27-30, doi:10.1038/ngeo724.

418 Prescott, C. L., A. M. Haywood, A. M. Dolan, S. J. Hunter, J. O. Pope, and S. J.
419 Pickering (2014), Assessing orbitally-forced interglacial climate variability during
420 the mid-Pliocene Warm Period, *Earth Planet. Sci. Lett.*, 400, 261-271,
421 doi:10.1016/j.epsl.2014.05.030.

422 Raymo, M. E., B. Grant, M. Horowitz, and G. H. Rau (1996), Mid-Pliocene warmth:
423 Stronger greenhouse and stronger conveyor, *Mar. Micropaleontol.*, 27(1-4), 313-
424 326, doi:10.1016/0377-8398(95)00048-8.

425 Rayner, N. A., D. E. Parker, E. B. Horton, C. K. Folland, L. V. Alexander, D. P. Rowell,
426 E. C. Kent, and A. Kaplan (2003), Global analyses of sea surface temperature, sea
427 ice, and night marine air temperature since the late nineteenth century. *J.
428 Geophys. Res.*, 108, doi:[10.1029/2002JD002670](https://doi.org/10.1029/2002JD002670), D14.

429 Reynolds, R. W., N. A. Rayner, T. M., Smith, D. C. Stokes, and W. Wang, 2002: An
430 Improved In Situ and Satellite SST Analysis for Climate, *J. Clim.*, 15, 1609-1625.

431 Robinson, M. M., P. J. Valdes, A. M. Haywood, H. J. Dowsett, D. J. Hill, and S. M.
432 Jones (2011), Bathymetric controls on Pliocene North Atlantic and Arctic sea
433 surface temperature and deepwater production, *Paleogeogr. Paleoclimatol.
434 Paleoecol.*, 309(1-2), 92-97, doi:10.1016/j.palaeo.2011.01.004.

435 Rosenbloom, N. A., B. L. Otto-Btiesner, E. C. Brady, and P. J. Lawrence (2013),
436 Simulating the mid-Pliocene Warm Period with the CCSM4 model, *Geosci.
437 Model Dev.*, 6(2), 549-561, doi:10.5194/gmd-6-549-2013.

438 Smethie, W. M., R. A. Fine, A. Putzka, and E. P. Jones (2000), [Tracing the flow of North
439 Atlantic Deep Water using chlorofluorocarbons](#), *J. Geophys. Res. Oceans*,
440 105(C16), 14297-14323.

441 Unger, N., and X. Yue (2014), Strong chemistry- climate feedbacks in the Pliocene,
442 *Geophys. Res. Lett.*, 41(2), 527-533, doi:10.1002/2013gl058773.

443 Wadley, M. R., and G. R. Bigg (2002), Impact of flow through the Canadian Archipelago
444 and Bering Strait on the north Atlantic and Arctic circulation: An ocean modelling
445 study, *Quart. J. Roy. Meteor. Soc.*, 128(585), 2187-2203, doi:10.1256/qj.00.35.

446 Zhang, Z. S., et al. (2013), Mid-pliocene Atlantic Meridional Overturning Circulation not
447 unlike modern, *Clim. Past*, 9(4), 1495-1504, doi:10.5194/cp-9-1495-2013.



Geophysical Research Letters

Supporting Information for

Amplified North Atlantic warming in the late Pliocene by changes in Arctic gateways

Bette L. Otto-Bliesner¹, Alexandra Jahn², Ran Feng¹, Esther C. Brady¹, Aixue Hu¹, and Marcus Löfverström¹

¹Climate and Global Dynamics Laboratory, National Center for Atmospheric Research, Boulder, CO 80305, USA.

²Dept. of Atmospheric and Oceanic Sciences and Institute for Arctic and Alpine Research, Univ. of Colorado Boulder, Boulder, CO 80309, USA.

Contents of this file

Text S1
Figures S1 to S2
Tables S1 to S2

Introduction

Details of the CCSM4 model are included in the Methods (Text S1) and a comparison of the SST, SSS, and mixed-layer depths simulated by CCSM4 to observations (Figure S1). Also included in the SI is a supplementary figure showing the annual Arctic sea ice distributions simulated in the PI and Pliocene experiments (Figure S2). Tables S1 and S2 provide supporting information for results described in the main text.

Text S1. Methods

The simulations for this study used the CCSM4 (Gent et al., 2011), which has active atmosphere, land, ocean, and sea ice component models that are linked through a coupler that exchanges state information and fluxes between the components. The atmosphere component model is the Community Atmosphere Model, version 4 (CAM4) and the land component is the Community Land Model, version 4 (CLM4). Both adopt the FV1 version, which has a horizontal resolution of 0.9° in latitude and 1.25° in longitude, respectively. The ocean and sea ice components are the Parallel Ocean Program, version 2 (POP2), and the Community Sea Ice Model, version 4 (CICE4), with common grid of 320 x 384 points, a displaced-pole grid with poles

in Greenland and Antarctica, and a nominal 1° resolution with finer resolution near the equator and North Atlantic. We adopt the alternate boundary conditions in our PlioMIP1 simulation. The PI simulation has been run for 1300 years; the PlioMIP1 simulation for 650 years, branching from the PI simulation at year 801 and with the ocean temperatures modified using the PRISM3 reconstructed SST and deep ocean temperature anomalies. The Pliocene gateways sensitivity experiments were started from year 451 of the PlioMIP1 simulation and run to year 650, except for CAA which was extended an additional 100 years to allow the AMOC to equilibrate. All results are shown for 50-year averages at the end of each simulation.

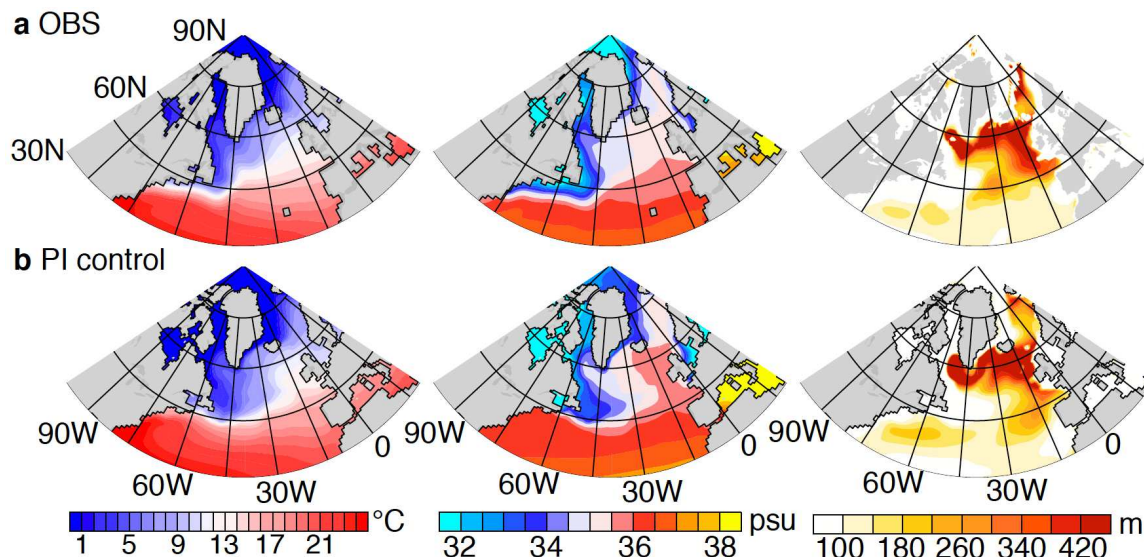


Figure S1. Comparison of SST (left), SSS (middle), and Mixed-layer Depths (right). (a) annual-mean SST ($^{\circ}$ C), SSS (psu) and winter (December to February) mixed layer depth [m] in observations (Monterey and Levitus, 1997; Locarnini et al., 2009; Antonov et al., 2010) and (b) the CCSM4 preindustrial (PI) simulation.

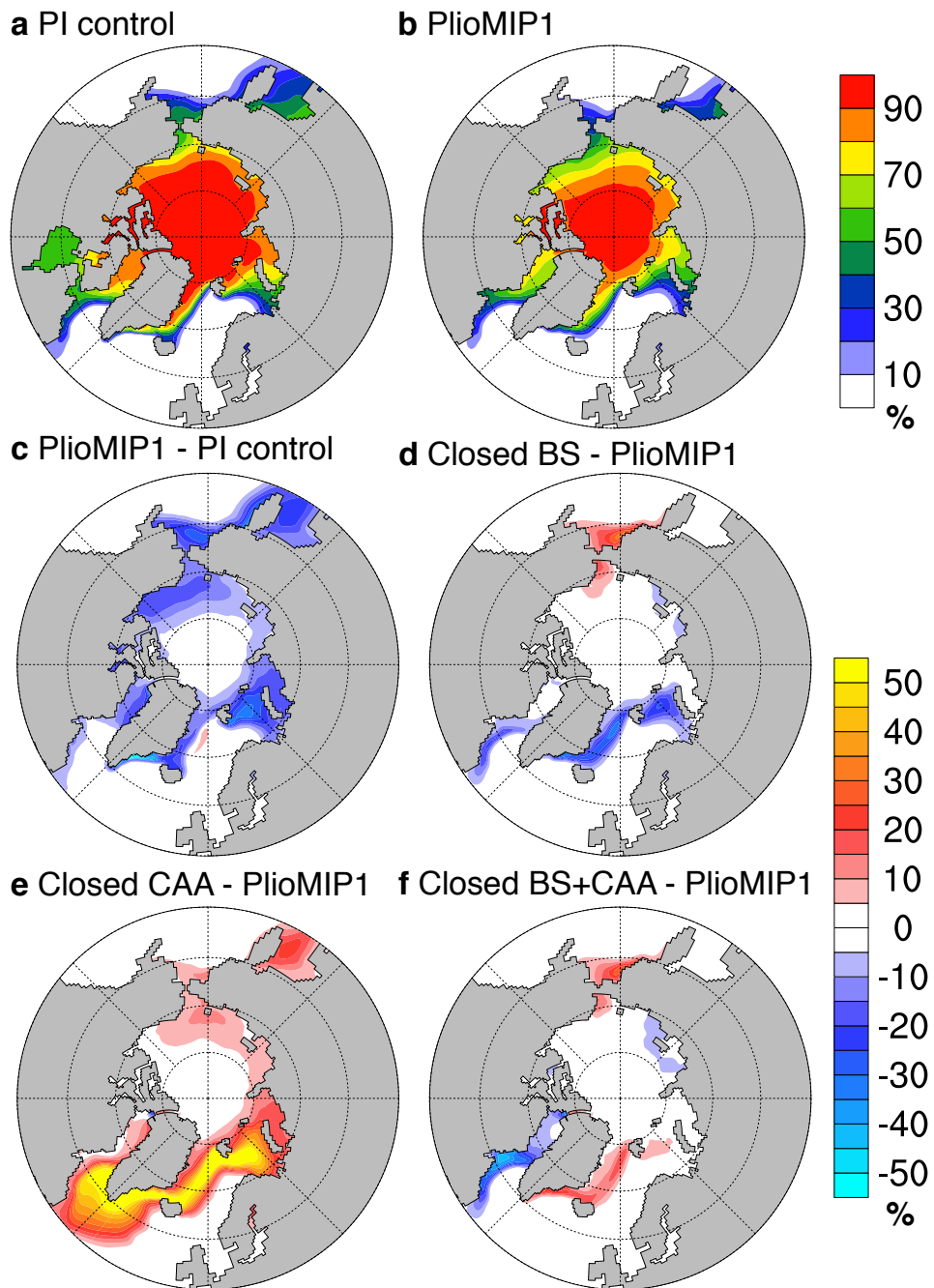


Figure S2. Comparison of Arctic sea ice concentrations (%) in CCSM4 simulations. a, Preindustrial simulation b, PlioMIP1 simulation. c, Change, PlioMIP1 minus preindustrial. d, e, f, Change as compared to the PlioMIP1 simulation for the Closed BS (d), Closed CAA (e), and Closed BS+CAA (f) experiments.

Sites	Lat	Lon	Conf	PRISM3	PlioMIP1	Closed BS	Closed CAA	Closed BS+CAA
DSDP_607	41.00	-32.96	4	-0.19	1.32	1.81	0.54	1.96
DSDP_608	42.84	-23.09	4	4.60	1.58	2.04	-0.30	1.96
DSDP_410	45.51	-29.48	3	4.30	0.67	2.15	-0.16	3.22
DSDP_609	49.88	-24.24	4	5.58	1.16	2.32	0.83	4.00
DSDP_111	50.43	-46.37	4	5.56	1.76	4.01	-1.86	5.49
DSDP_610	53.22	-18.89	4	6.61	1.41	2.28	-1.29	2.66
DSDP_552	56.04	-23.23	4	5.85	1.69	2.55	-3.00	2.84
DSDP_548	48.85	-12.00	4	8.79	1.31	1.96	-0.91	1.87
ODP_907	69.25	-12.70	3	9.44	1.25	5.04	-8.98	-0.98

Table S1. Mid- and high-latitude SST anomalies (°C) in North Atlantic region in PRISM3

reconstruction and Pliocene simulations. Sites are those with high (3) or very high (4) confidence levels from Dowsett et al., 2012, 2013. Confidence levels (Conf, increasing confidence from level 1 to 4) are provided by Dowsett et al., 2012 based on semi-quantitative assessments of proxy age control, number of samples, abundance and preservation of fossils, and reliability of reconstruction methods,. Model anomalies are Pliocene simulations minus preindustrial. Preindustrial (Rayner et al., 2003) minus present-day SST (Reynolds et al., 2002) corrections are added to the PRISM3 SST anomalies to ensure the consistency of data-model comparison.

	PlioMIP1	Closed BS	Closed CAA	Closed BS+CAA
Total net Arctic FW inputs	11013	7748	10608	7733
Bering Strait				
Liquid	3149	0	2957	0
Solid (ice)	151	0	200	0
River runoff	4981	5077	4649	5058
P-E	2732	2671	2802	2675
Total net Arctic FW exports	-10377	-7241	-9712	-7387
CAA				
Liquid	-5123	-3148	0	0
Solid (ice)	-650	-528	0	0
Fram Strait				
Liquid	-2011	-938	-5413	-4192
Solid (ice)	-1718	-1323	-3072	-2252
Barents Sea				

Liquid	-841	-1298	-661	-883
Solid (ice)	-34	-6	-566	-60
Total net Solid FW export	-2402	-1857	-3638	-2312
Total net Liquid FW export	-7975	-5384	-6074	-5075

Table S2. Annual means of the net Arctic Ocean freshwater (FW) fluxes from Pliocene simulations. All oceanic fluxes (km^3/yr) are net fluxes over the full depth of the water column at the boundaries. FW fluxes are calculated using monthly means relative to a reference salinity of 34.8 psu, with negative numbers indicating net FW exports from the Arctic Ocean, and positive numbers indicating net FW inputs. Small imbalances between total net Arctic FW inputs and outputs are associated with several factors including only calculating over a 50-year period for each experiment and using monthly means of velocity and salinity in the calculations.